A quantitative diffuse reflectance spectroscopy study of chromium-containing zeolites

Bert M. Weckhuysen, Hans J. Spooren, and Robert A. Schoonheydt
Centrum voor Oppervlaktechemie en Katalyse, K.U.Leuven, Heverlee, Belgium.

The diffuse reflectance spectra of chromium-containing zeolites (Y, GaY, X, and mordenite) have been investigated before and after drying, after calcination, after successive CO reduction, and after recalcination. Different methods of Cr zeolites preparation (ion exchange, solid-state ion exchange, and impregnation) were investigated. A method for quantifying Cr(VI) ions was developed. Before and after drying, Cr(III) is octahedrally coordinated, which is almost quantitatively oxidized upon calcination at 550°C to Cr(VI). Cr(VI) is a chromatelike species with two lattice and two extralattice oxygens in the coordination sphere. The Cr dispersion depends on the zeolite type and preparation method. The reducibility of Cr(VI) to Cr(III) and Cr(II) follows the order Cr mordenite > CrY (impregnated) > CrY (ion exchange) > CrX > CrGaY > CrY (solid state). This order can be qualitatively explained in terms of zeolite properties and Cr dispersion.

Keywords: Cr zeolites; ion exchange; redox behavior; DRS

INTRODUCTION

Cr zeolites are known to possess, at least on the laboratory scale, important catalytic properties like ethylene polymerization,[1,2] oxidation of hydrocarbons,[3] CH_2Cl_2,[4,5] H_2, NH_3, and CO,[3,6] cracking of cumene,[7] disproportionation of *n*-heptane,[7] isomerization of methyl-3-pentane,[7] and thermolysis of H_2O.[8] The catalytic properties of Cr-containing zeolites depend on the reaction temperature, the structure of the zeolite, and the oxidation state and coordination of the Cr ions.

These Cr zeolites can be prepared in three different ways: ion exchange, impregnation, and solid-state ion exchange. Whatever the preparation method, it is believed that different oxidation states of Cr, in particular, Cr(VI), Cr(V), Cr(III), and Cr(II), can be stabilized in zeolite structures, each with their specific coordination geometry.[9] After ion exchange, $Cr(H_2O)_6^{3+}$ or $Cr(H_2O)_6^{2+}$ ions are present in the cavities and/or channels and these ions migrate to cationic sites on the surface after dehydration. Pearce and Mortier showed by X-ray diffraction (XRD) that Cr(III) ions are located at the three-coordinated site I′ in dehydrated faujasite structures, at least at relatively high Cr loadings.[10] Solid-state ion exchange followed by calcination results in the migration of Cr into the zeolite channels and cavities, where it is present as Cr(VI) and Cr(V). Reduction results in the formation of Cr(V), Cr(III), and Cr(II), but Cr(O) is also claimed.[11]

With the aid of diffuse reflectance spectroscopy (DRS), different oxidation states [Cr(VI), Cr(III), and Cr(II)] and coordinations can be detected, and therefore, this technique is an excellent tool for studying Cr catalysts. Up to now, DRS studies have been qualitative. *Table 1* gives a survey of reported DRS absorption bands and proposed assignments. The data of the different research groups cannot be easily compared because of different loadings and pretreatments. Furthermore, no DRS data are available of (1) reduced Cr zeolites and (2) Cr zeolites prepared by solid-state ion exchange and impregnation.

The purpose of this work was a systematic quantitative study of Cr-containing zeolites by DRS. We studied the effect of the zeolite composition, structure, and method of preparation. These effects will be evaluated before and after drying, after calcination, successive CO reduction, and recalcination. Quantitative measurements of Cr species by DRS are possible for amorphous supports.[21] They allow a more thorough discussion of the chemistry of Cr.

EXPERIMENTAL

Sample preparation and characteristics

NaX and NaY (Ventron), Na mordenite (Norton), and NaGaY (Exxon Research) were put in their Na^+ form by two successive exchanges with 1 M NaCl solutions, washed Cl^- free, and dried in air at room

Address reprint requests to Mr. Weckhuysen at the Centrum voor Oppervlaktechemie en Katalyse, K.U.Leuven, Kardinaal Mercierlaan 92, B-3001 Heverlee, Belgium.
Received 11 November 1993; accepted 14 February 1994

Table 1 Literature survey of DRS absorption bands of Cr-exchanged zeolites and their assignments

Sample	Sample pretreatment	Absorption bands (cm^{-1})	Assignments[a]	Ref.
Cr(II)/NaA (1–3 Cr/u.c.)	Hydrated	12,000; 17,000	Cr^{2+}_{trig}	12
Cr(III)/NaL (1.33 Cr/u.c.)	Hydrated	17,400; 25,000; 35,800	$Cr(H_2O)^{3+}_6$	13
	Dehydrated	15,000	Cr^{3+}_{oct}	
	Calcined	27,100; 34,000	CrO^{2-}_4	
Cr(III)/Na mordenite (1.56 Cr/u.c.)	Hydrated	17,200; 24,600; 35,800	$Cr(H_2O)^{3+}_6$	13
	Dehydrated	15,000	Cr^{3+}_{oct}	
	Calcined	26,800; 36,500	CrO^{2-}_4	
Cr(III)/NaY (3.9 Cr/u.c.)	Hydrated	17,200; 23,800	$Cr(H_2O)^{3+}_6$	14
	Calcined	13,900; 28,600	Cr^{6+}	
Cr(III)/NaX (4.3 Cr/u.c.)	Hydrated	17,200; 23,800	$Cr(H_2O)^{3+}_6$	14
	Calcined 300°C	13,900; 28,600	Cr^{6+}	
Cr(III)/NaY	Hydrated	17,200; 24,400	$Cr(H_2O)^{3+}_6$	15
	Dehydrated 350°C	13,300	Cr^{2+}	
Cr(III)/NaY (0.39 Cr/u.c.)	Dehydrated 20°C	16,100; 23,800	$Cr(H_2O)^{3+}_6$	16
	Dehydrated 100°C	15,900; 23,100	Cr^{3+}_{oct}	
	Dehydrated 200°C	8,000; 9,100; 15,600; 20,800	Cr^{3+}_{tetr}; Cr^{3+}_{oct}	
Cr(II)/NaY (1.5 Cr/u.c.)	Hydrated	14,000	$Cr(H_2O)^{2+}_6$	17
	Dehydrated 350°C	12,300; 17,000	Cr^{2+}_{trig}	
Cr(III)/NaA, NaX, and NaY	Hydrated	16,000; 23,550; 35,100	$Cr(H_2O)^{3+}_6$	18
Cr(II)/NaY	Hydrated	13,500	$Cr(H_2O)^{2+}_6$	19
	Dehydrated 300°C	12,600; 15,200; 31,000	$Cr^{2+}_{distoct}$	
Cr(III)/NaY (4, 8, 15.8 Cr/u.c.)	Hydrated	17,100; 23,800	$Cr(H_2O)^{3+}_6$	20
	Calcined 550°C	17,100; 22,200; 27,800; 37,700	Cr^{3+}_{oct}; CrO^{2-}_4	
	Dehydrated 450°C	14,200; 16,400; 22,400	Cr^{3+}_{oct}	

[a] trig = trigonal; oct = octahedral; tetr = tetrahedral; distoct = distorted octahedral

temperature overnight. The zeolites were then ion-exchanged with a solution of $CrCl_3 \cdot 6\ H_2O$ during 2 h at room temperature. After ion exchange, the samples were separated from the solution by centrifugation, washed Cl^--free, and dried at 60°C overnight in air. Cr-impregnated NaY was prepared by the incipient wetness method with $CrCl_3 \cdot 6\ H_2O$, using the NaY from Ventron. The samples were dried at 60°C overnight. Cr/Al_2O_3 was prepared as previously described.[21] The HY zeolite was made from the NaY zeolite by ion exchange with a NH_4^+ solution, followed by calcination at 550°C overnight in air. $CrCl_3 \cdot 6\ H_2O$ and HY were mixed in a mortar until a homogeneous color was obtained. The ion-exchanged, impregnated, and solid-state ion-exchanged samples are indicated by, respectively, the symbols IE, IMP, and SOL (*Table 2*). The anhydrous unit cell composition of the used zeolites are summarized in *Table 2*, together with the Cr contents, determined by atomic absorption spectrometry (AAS) after dissolution of known quantities of the samples in HF/H_2SO_4. The amounts of Cr of the samples are expressed as wt% or number of Cr atoms per u.c.

Table 2 Cr content of the samples

Support type[a]	Sample name	Cr content
NaY $[Na_{55}Al_{55}Si_{137}O_{384}]$	NaYIE1	0.089 Cr/u.c.
	NaYIE2	0.20 Cr/u.c.
	NaYIE3	0.38 Cr/u.c.
NaGaY $[Na_{58}Ga_{58}Si_{134}O_{384}]$	GaYIE1	0.32 Cr/u.c.
	GaYIE2	0.55 Cr/u.c.
	GaYIE3	1.11 Cr/u.c.
NaX $[Na_{84}Al_{84}Si_{107}O_{384}]$	NaXIE1	0.093 Cr/u.c.
	NaXIE2	0.19 Cr/u.c.
	NaXIE3	0.34 Cr/u.c.
Na mordenite $[Na_{0.5}Al_{0.5}Si_{47.5}O_{96}]$	NaMordIE1	0.14 Cr/u.c.
	NaMordIE2	0.23 Cr/u.c.
	NaMordIE3	0.31 Cr/u.c.
NaY $[Na_{55}Al_{55}Si_{137}O_{384}]$	NaYIMP1	0.087 Cr/u.c.
	NaYIMP2	0.18 Cr/u.c.
	NaYIMP3	0.37 Cr/u.c.
HY $[H_{39}Na_{16}Al_{55}Si_{137}O_{384}]$[b]	HYSOL1	0.09 wt%
	HYSOL2	0.28 wt%
	HYSOL3	0.56 wt%
Al_2O_3	Cr/Al_2O_3	0.49 wt%

[a] Anhydrous unit cell composition
[b] Estimation of the H^+ content (70% of Na^+ are replaced by H^+)

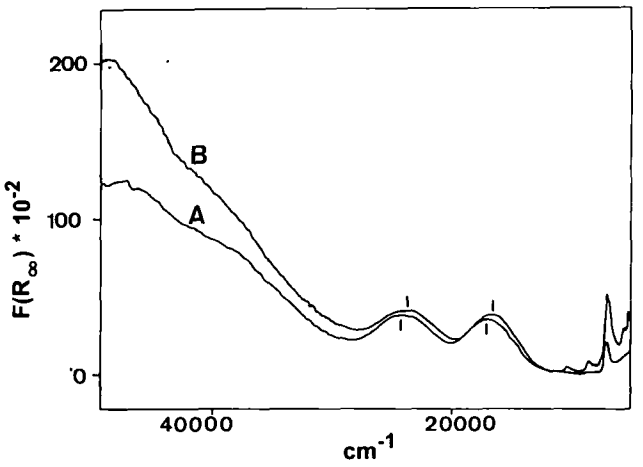

Figure 1 DRS spectra of GaYIE3 (A) as such and (B) after drying.

Pretreatment and experimental techniques

After preparation and drying, the samples were granulated. The size fraction 0.25–0.4 mm was loaded in a quartz flow cell with suprasil window for DRS. DRS spectra were taken of the samples as such and after drying at 75°C overnight. Subsequently, the samples were calcined at 550°C during 4 h and then reduced with CO at 200, 300, 400, and 600°C during 30 min. DRS spectra were recorded on these calcined samples and after each reduction step. After reduction, the samples were recalcined in oxygen during 4 h at 550°C and DRS spectra were taken again.

DRS spectra were taken with a Varian Cary 5 u.v.-vis-n.i.r. spectrophotometer at room temperature. The spectra were recorded against a halon white reflectance standard in the range 2200–200 nm. The computer processing of the spectra consisted of the following steps: (1) subtraction of the base line; (2) conversion to wavenumber; and (3) calculation of the Kubelka–Munk (KM) function. The spectra were deconvoluted into Gaussian bands with the Spectra Calc program of Galactic Industries. The values of the KM function at the band maxima were used for quantitative DRS. X-ray diffractograms were measured using an automated Siemens diffractometer, equipped with a Kristalloflex K710 röntgengenerator and a position sensitive detector of Inel. ^{27}Al *MAS* n.m.r. spectra were taken using a Bruker MSL 400 spectrometer at 104.2 MHz in a magnetic field of 9.4 T, with a tipping angle of 15° and a spinning frequency of 14.5 kHz. Three thousand scans were accumulated. ^{29}Si *MAS* n.m.r. spectra were measured at 79,460 MHz under the same conditions with a spinning frequency of 4 kHz. AAS measurements were performed using an Instrumentation Laboratory Inc. apparatus with a nitrous oxide–acetylene flame. The light source was a hollow cathode lamp with a wavelength of 357.9 nm.

RESULTS

XRD diffractograms and ^{27}Al and ^{29}Si *MAS* n.m.r. spectra were measured on the freshly prepared and recalcined samples. The spectra indicate that the crystallinity of the zeolites was unaffected and that no extralattice Al was formed during the treatments.

Hydrated and dried samples

Freshly prepared Cr-exchanged zeolites are green and the DRS spectra are dominated by three absorption bands: 17,000, 24,000, and 33,000 cm^{-1}, typical for $Cr(H_2O)_6^{3+}$. Representative spectra are shown in *Figure 1* for GaYIE1 before and after drying. The 33,000 cm^{-1} band is present only as a broad shoulder on the background. Drying shifts the first two absorption bands slightly to the red, and as a consequence, the ligand field is decreased. This is in accordance with earlier work of Coughlan et al.[13] The bands in the n.i.r. region are overtones and combination bands of water.

Calcined samples

After calcination, the color of the samples is yellow and the spectra are shown in *Figure 2*. Three types of DRS spectra are observed: CrX, CrGaY, and Cr mordenite are characterized by the DRS spectra of *Figure 2A*. These spectra are dominated by two bands, one at 28,000 and a broad band in the region 38,000–39,000 cm^{-1}, typical for chromate species. Ion-exchanged and impregnated Y-type zeolites have, in addition, a clear shoulder at 22,500 cm^{-1} (*Figure 2B*). This shoulder is attributed to the presence of dichromate (and/or polychromates).[21] The DRS spectra of solid-state-exchanged Cr zeolites have an additional weak low frequency band at 10,000 cm^{-1} (*Figure 2C*). The spectra of the calcined materials can be decomposed in Gaussian components following an earlier described procedure.[21] An example is shown in *Figure 3* for GaYIE2. The spectra are decomposed into four bands of chromate (23,500, 28,000, 34,100, and 38,500 cm^{-1}), three weak bands of octahedral Cr(III) (15,900, 24,100, and 33,000 cm^{-1}), and a support band (47,000 cm^{-1}). The four

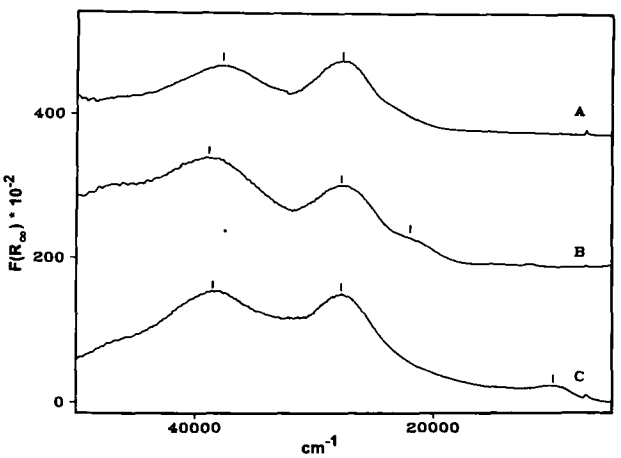

Figure 2 DRS spectra of calcined Cr zeolites: (a) CrX, CrGaY, and Cr mordenite; (b) CrY (impregnated and ion-exchanged); (c) CrY (solid state).

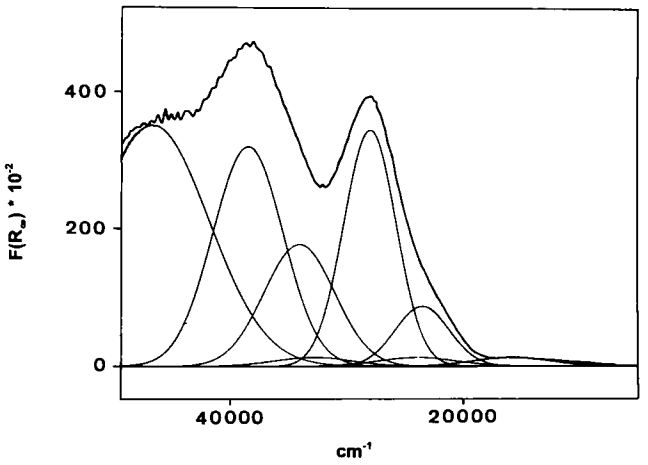

Figure 3 Deconvoluted DRS spectrum of calcined GaYIE2.

bands of Cr(VI) are typical charge-transfer bands of metallochromates and are assigned to $1t_1 \rightarrow 2e$ (23,500 cm^{-1}), $1t_1 \rightarrow 2e$ (28,000 cm^{-1}), $1t_1 \rightarrow 7t_2$ (34,100 cm^{-1}), and $6t_2 \rightarrow 2e$ (38,500 cm^{-1}).[21] The first band is spin-forbidden, whereas the other bands are spin-allowed. The weak *d–d* transitions of Cr(III) are only revealed by decomposition.

Reduced and recalcined samples

Qualitative DRS spectroscopy

Reduction is characterized by a decrease of the O → Cr(VI)–CT bands and starts above 200°C, except for mordenite, for which it starts around 150°C. We will describe as an example the spectra of the GaYIE2 more in detail (*Figure 4*). The intense bands at 28,000 and 38,000 cm^{-1}, typical for Cr(VI), are decreasing with increasing reduction temperature at the expense of absorptions in the *d–d* region. A weak band of Cr(III) becomes visible at 16,000 cm^{-1} and grows in intensity with reduction temperature. This band is asymmetric toward lower wavenumbers, suggesting low-frequency components.

A proposal for the deconvolution of the GaYIE2 spectra is shown in *Figure 5*. All the spectra of the reduced samples (reduction temperature > 200°C) can be decomposed in four chromate bands, three bands of octahedral Cr(III), and two bands at around 12,600 and 7,600 cm^{-1}. The latter two bands can be tentatively assigned to, respectively, Cr(II) ions in octahedral and tetrahedral coordination[21] and become visible, especially after reduction at 300 and 400°C.

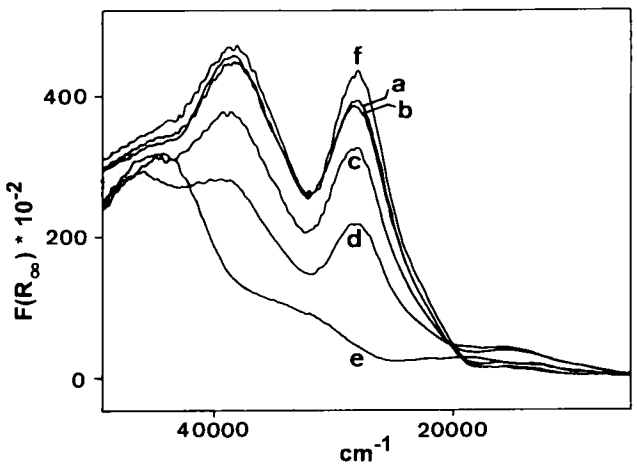

Figure 4 DRS spectra of NaGaYIE3: (A) reduction 200°C; (B) reduction 300°C; (C) reduction 400°C; (D) reduction 600°C; (E) recalcination 550°C.

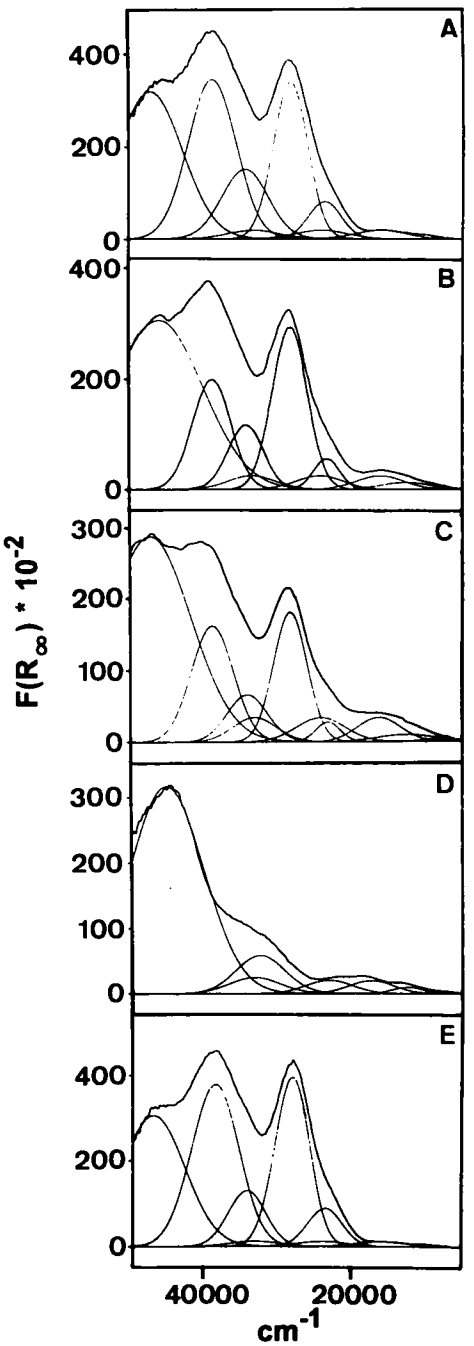

Figure 5 Deconvolution of the DRS spectra of GaYIE2: (A) reduction 200°C; (B) reduction 300°C; (C) reduction 400°C; (D) reduction 600°C; (E) recalcination 550°C.

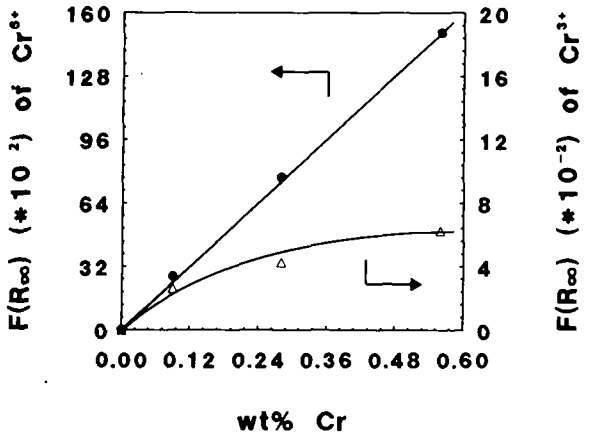

Figure 6 Calibration lines for Cr/HY solid state.

All Cr zeolites behave spectroscopically as described above. However, the spectra of Cr mordenite and Cr/HY (solid state) are different in the following features: The spectra of Cr mordenite show a broad adsorption band in the *d–d* region at around 15,000 cm^{-1}, which has its maximum after reduction at 300°C. With higher reduction temperature, the intensity decreases but the absorption band remains at the same position. The Cr/HY (solid state) zeolite shows an increase of the band at around 10,000 cm^{-1} with reduction temperature until a maximum is attained at 400°C.

After reduction at 600°C, the overall intensity of the DRS spectra of all Cr zeolites is significantly decreased, suggesting that not all Cr is contributing to the DRS spectra. The exceptions are the solid-state-exchanged Y zeolites, which retain a broad 15,000 cm^{-1} with shoulder at 19,500 cm^{-1} after reduction at 600°C.

After complete disappearance of the chromate bands, new bands become apparent in the region 30,000–40,000 cm^{-1}: one weak band at 33,000 cm^{-1} and a second stronger band around 40,000 cm^{-1}. Finally, all samples have a broad band above 40,000 cm^{-1} which is due to the support.

After recalcination of the reduced samples, a yellow color reappears. The spectra are the same as those of the calcined materials, suggesting a reversible redox process.

Quantitative DRS spectroscopy

The KM function allows a quantitative determination of absorbing species according to:

$$F(R_\infty) = \frac{(1 - R_\infty)^2}{2R_\infty} = \frac{K}{S} = \frac{\alpha C_{Cr}}{S} = kC_{Cr} \qquad (1)$$

where R_∞ is the ratio of the light intensity reflected from the sample and the light reflected from the standard.[22] K and S are, respectively, the KM absorption and scattering coefficients. When, at a given wavelength, S is constant, Equation (1) gives a linear relation between $F(R_\infty)$ and the Cr concentration, C_{Cr}. Conditions inherent to the use of the KM function are (1) an infinitely thick sample, (2) random distribution of particles that are much smaller than the layer thickness, (3) isotropic scattering and diffuse irradiation, and (4) samples with low absorption.

The first, second and third conditions are fulfilled by using powdered samples, whereas the fourth condition suggests the use of low Cr loadings. It is also assumed that S does not change with loading and treatment.

In the following procedure, calibration lines are obtained for Cr(III) and Cr(VI). In calcined Cr-containing zeolites, Cr(VI) is present mainly as chromate and the Cr(VI) calibration lines are obtained by plotting the intensity of the 28,000 cm^{-1} band of chromate as a function of the Cr loading. The Cr(III) calibration lines were obtained by plotting the intensity of the 16,000 cm^{-1} band of the dried Cr(III)-exchanged samples as a function of the Cr loading. An example of calibration lines is shown in *Figure 6* for the Cr solid-state-exchanged Y zeolites. A straight Cr(VI) calibration line is obtained and this is the case for all calcined samples except for CrGaY. The Cr(III) calibration lines are not linear. Therefore, we restrict the quantitative analysis to Cr(VI). The relative concentrations of Cr(VI) after different pretreatments are shown in *Figure 7*. It shows that (a) CO reduction starts above 200°C, except for Cr/Na mordenite, (b) the amount of chromate is zero after reduction at 600°C, except for Cr/HY (solid state), and (c) the relative decrease of Cr(VI) in the region 200–600°C, when used as a reducibility criterion, follows the sequence Cr/HY < Cr/NaGaY < Cr/NaX < Cr/Nay (ion exchange) < Cr/NaY (impregnation) < Cr/Na mordenite, and (e) after recalcination, all the chromate is reestablished.

When, at a given reduction temperature, the relative amount of Cr(VI) is followed as a function of time, the data of *Figure 8* are obtained. For Cr/Al_2O_3,

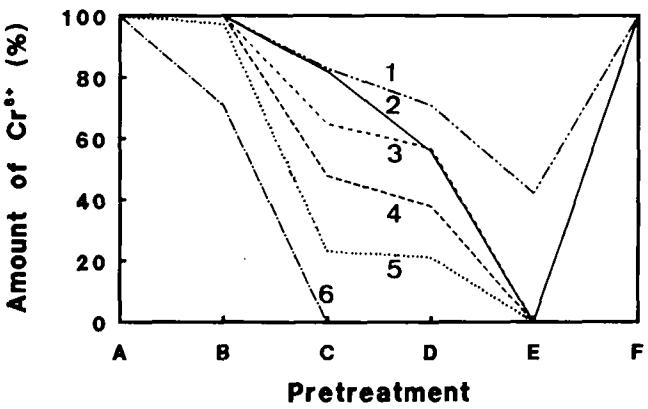

Figure 7 Amount of Cr(VI) as function of different pretreatments: (A) calcination 550°C; (B) reduction 200°C; (C) reduction 300°C; (D) reduction 400°C; (E) reduction 600°C; (F) recalcination 550°C; and zeolites: (1) Cr/HY solid state; (2) Cr/GaY; (3) Cr/NaX; (4) Cr/NaY ion exchange; (5) Cr/NaY impregnation; (6) Cr/Na mordenite.

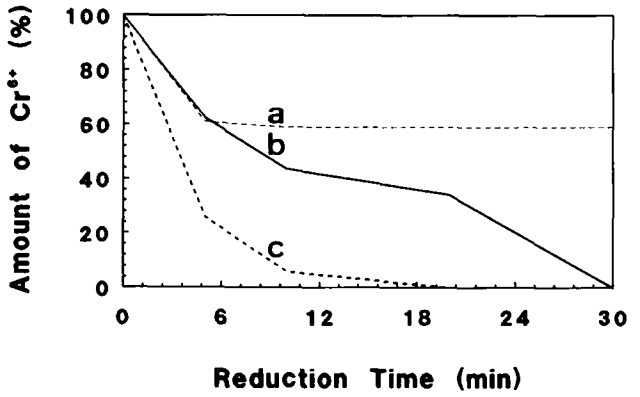

Figure 8 Amount of Cr(VI) as function of time: (a) NaYIE2 reduced at 410°C; (b) NaYIE1 reduced at 550°C; (c) Cr/Al_2O_3 reduced at 380°C.

all Cr(VI) can be reduced at 380°C with an apparent pseudo-first-order rate ($k = 0.0046\ s^{-1}$). For NaYIE1, the reduction is a two-step process both at 410 and 550°C. In the first step, about 40% of the Cr(VI) is easily reduced at 410°C, whereas at 550°C, about 60% is reduced. Reduction of the remaining 40% starts after 18 min reduction time at 550°C.

DISCUSSION

The chemistry of Cr(N) (with N = II, III, or VI) in zeolites is the same whatever the loading, the type of immobilization, and the structure type. Upon calcination, chromate species are formed that, upon reduction with CO, transform to Cr(III) with some Cr(II) and undetected Cr in some cases; recalcination restores the initial chromate composition. This, together with the XRD and ^{27}Al and ^{29}Si *MAS* n.m.r. data, suggests that, within the accuracy of the methods, the redox behavior of Cr zeolites is reversible. The details of the chemistry outlined above are zeolite-dependent and merit a more detailed discussion. This discussion will cover the following topics: (1) spectroscopy of Cr and (2) redox chemistry of Cr.

Spectroscopy of Cr

With DRS spectroscopy in the u.v.-vis-n.i.r., we probe the charge-transfer and *d–d* transitions of Cr. The charge-transfer transitions are of the type O → Cr(VI) and are typical for Cr(VI) in chromate, dichromate, and polychromates. Cr(II) and Cr(III) have characteristic *d–d* transitions, which are much weaker than the charge transfers. In any case, both types of absorptions are characteristic for the oxidation state of Cr and for the nature and geometry of the atoms in the coordination sphere, in our case oxygens. Long-range effects, for instance the distinction between monomeric chromate and polymeric chromate, cannot be made directly. Therefore, our results do not allow making firm conclusions on the degree of the polymerization of Cr in zeolites.

Hydrated and dried samples

After ion exchange and impregnation, Cr(III) ions are present as hexa-aquo complexes in the supercages of Y-type zeolites and in the main channels of mordenite. Drying results in a small decrease of the ligand field strength of the $Cr(H_2O)_6^{3+}$ complex, as evidenced by the red shift of the *d–d* bands. This lowering is due to two phenomena: (a) the removal of water from the second coordination sphere of chromium and (b) the replacement of one (or more) water molecule(s) in the first coordination sphere of the Cr(III) ion by a weaker ligand, e.g., the lattice oxygen of the zeolite. This process can be visualized in the following way:

$$Cr(H_2O)_6^{3+} + n\ {}^{-}O\text{–Zeo} \rightarrow Cr^{3+}\text{–}(O\text{–Zeo})_n(H_2O)_m + (6\text{–}m)\ H_2O \quad (2)$$

The location and nature of the Cr-complexes after impregnation and mixing with solid $CrCl_3 \cdot 6\ H_2O$ is not known but appreciable quantities of Cr may be on the external surface.

Calcined samples

Chromate, "CrO_4^{2-}," is found in all zeolites after calcination. Only in the case of ion-exchanged and impregnated CrY were dichromate (or polychromate) species clearly found, as evidenced by the 22,500 cm^{-1} shoulder. This indicates less dispersion. In most cases, calcination is also accompanied by formation of small amounts of Cr_2O_3 with a characteristic *d–d* transition around 16,000 cm^{-1}.

The formation of chromate holds also for the solid-state-exchanged zeolite. This can be modeled as a two-step process:

$$CrCl_3 + 3\ H\text{–}O\text{–Zeo} \rightarrow Cr^{3+}(\text{–}O\text{–Zeo})_3 + 3\ HCl\uparrow \quad (3)$$

$$Cr^{3+}(\text{–}O\text{–Zeo})_3 + O_2 \rightarrow \text{"}CrO_4^{2-}\text{"} + 3\ {}^{-}O\text{–Zeo} \quad (4)$$

The anionic chromate is not likely to be electrostatically stabilized by the negatively charged framework. Three processes can be envisaged:

1. Calcination results in the formation of protons, which neutralize both the chromate and the zeolite framework. The reaction can be envisaged as:

$$Cr^{3+}(\text{–}O\text{–Zeo})_3 + 3/4\ O_2 \rightarrow + 5/2\ H_2O \rightarrow H_2CrO_4 + 3\ H\text{–}O\text{–Zeo} \quad (5)$$

   Thus, chromate is a neutral species, which likely transforms to Cr_2O_3 clusters. The absence of large amounts of Cr_2O_3 after calcination suggests that this process only occurs to a limited extent.
2. Cr(VI) with an ion radius of 52 pm can substitute for Al(III) (51 pm) in the framework. This creates locally an excess positive charge and extralattice Al. We did not find evidence for extralattice Al by *MAS* n.m.r. or for structural breakdown by XRD. This is not sufficient to reject this hypothesis

totally, but, nevertheless, we think that such a substitution is unlikely because of the charge difference between Cr(VI) and Al(III).

3. The chromate species is anchored to two oxygen atoms of the zeolite. This reaction results in the formation of two extraframework oxygens and can be depicted as:

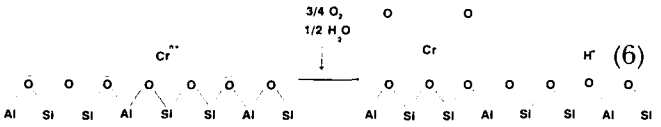

(6)

For charge neutrality reasons, this anchoring requires two structural oxygens, each bound to one Al(III). This hypothesis is the most likely one. The same anchoring mechanism is proposed for chromium on amorphous supports.[21,23]

Reduced samples

Cr(VI) in calcined Cr zeolites can be reduced by CO, and the reduction reaction may be schematically envisaged as:

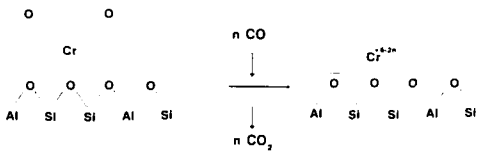

(7)

with n depending on the reduction temperature and time, the zeolite composition and type, and the preparation method.

The following criteria must be fulfilled for quantification of Cr(VI) during CO reduction: (1) a low Cr content and (2) the absence of Cr(III) in the calcined samples. These factors are fulfilled for Cr/HY (solid state), Cr/NaY (ion exchange), Cr/NaY (impregnation), Cr/NaX, and Cr mordenite. This is not the case for Cr/GaY; however, one can quantify also Cr(VI) for the lowest Cr loading of this sample. Recalcination completely regenerates the spectra of the calcined samples, suggesting a reversible redox process.

Redox chemistry of Cr

The rate of decrease of the amount of Cr(VI) with reduction temperature can be used as a measure for the reducibility of Cr. From *Figure 7*, it follows that the reducibility of Cr is decreasing in the following order: Cr mordenite > CrY (impregnated) > CrY (ion exchange) > CrX > CrGaY > CrY (solid state). These differences in redox behavior of Cr can be explained in terms of zeolite properties and Cr dispersion.

It is known that the harder the support the less susceptible the framework is for electron fluctuations, which are necessary for reductions. Thus, the harder the zeolite, the more difficult the reduction. The hardness of the zeolites is increasing when (1) the Al content increases[24] and (2) Al is changed by Ga.[25] Therefore, the hardness increases from Cr mordenite over CrY and CrX to CrGaY and, therefore, our hypothesis is qualitativly valid. The low reducibility of CrY (solid state) can be explained by the residual acidity of this sample. It is known that acidity retards reduction and the amount of bridging hydroxyls might be the highest on the CrY (solid state), because only a small amount of OH groups have been replaced by Cr.

However, during solid-state exchange, small amounts of Al can be released from the framework, which may combine with Cr to form relatively stable Cr–Al compounds. Their presence is indicated by the difficult reduction of Cr(VI). The amount must, however, be small, as no extralattice Al was detected by *MAS* n.m.r. Finally, the order of reducibility can be related to differences in dispersion of Cr(VI) in the different zeolites. On the impregnated Y zeolites, the 22,500 cm^{-1} band is indicative of dichromates or larger Cr(VI) clusters. They are more easily reduced, also because these clusters are probably partially located at the external surface.

In comparison with Cr supported on alumina, Cr is more difficult to reduce in zeolites. The reduction of Cr in ion-exchanged Y zeolites is a two-step process: In the first step, 40–60% of the Cr(VI) is reduced depending on the reduction temperature. The remaining Cr(VI) can only be reduced at high temperatures. Two effects are combined in this behavior, illustrated in *Figure 8*: (1) the distribution of Cr(VI) over supercages, cubo-octahedra, and hexagonal prisms and (2) the dispersion of Cr(VI). If all Cr(VI) is atomically dispersed, the reducibility is expected to follow the order supercage > cubo-octahedron > hexagonal prism. At low temperatures, only supercage Cr(VI) will be reduced, and as the temperature increases, those of cubo-octahedra and hexagonal prisms will be reduced also. If, in addition part of Cr(VI) is clustered, then for the same cavity, the reducibility follows the order clustered Cr(VI) > atomically dispersed Cr(VI). If a combination of atomically dispersed Cr(VI) and clustered Cr(VI) exists, the reducibility according to cavities will remain, and only the amount reduced in the first and second steps will change. Thus the two-step process is indicative of a distribution of Cr(VI) over cavities in the zeolite.

CONCLUSIONS

The main conclusions from this study are that

1. The deconvolution of the DRS spectra of Cr containing zeolites allows a quantitative determination of Cr(VI) provided that the loadings are low and there is no (or only a small quantity) of Cr(III) after calcination.
2. The redox behavior of Cr is dependent on the zeolite properties and Cr structure. The following sequence of increasing reducibility was obtained: CrY (solid state) < CrGaY < CrX < CrY (ion exchange) < CrY (impregnation) < Cr mordenite. Therefore, zeolites are playing an active role in the redox chemistry of Cr in zeolites. The harder the zeolite, the lower the reducibility of Cr(VI). This Cr(VI) exists as a chromatelike species in

zeolites and its reduction by CO proceeds via two steps.

ACKNOWLEDGEMENTS

B.M.W. acknowledges a grant as research assistant from the Belgian National Fund of Scientific Research (N.F.W.O.). The authors thank Piet Grobet and Hilde Geerts for the *MAS* n.m.r. measurements; Jan Uytterhoeven for the use of the Spectra Calc program; Herman Bosmans and Lut Ooms for the chemical analyses of the samples; and Hans Verduyn and Wilfried Mortier for the supply of the GaY zeolite. This work was financially supported by the Fonds voor Kollectief Fundamenteel Onderzoek (FKFO) under Grant No. 2.0050.93.

REFERENCES

1 Yashima, T., Nagata, J.-I., Shimazaki, Y. and Hara, N., in *Molecular Sieves – II* (Ed. J.R. Katzer) American Chemical Society, Washington, DC, 1977, p. 626
2 Yashima, T., Namba, S., Komatsu, T., Wang, J.-K. and Uematsu, T. *J. Mol. Catal.* 1986, **37**, 327
3 Tagiev, D.B. and Minachev, K.M. *Uspekhi Khim.* 1981, **50**, 1929
4 Chatterjee, S. and Greene, H.L. *J. Catal.* 1991, **130**, 76
5 Chatterjee, S., Greene, H.L. and Park, J.Y. *J. Catal.* 1992, **138**, 179
6 Kubo, T., Tominaga, H. and Kunugi, T. *J. Chem. Soc. Jpn.* 1973, **46**, 3549
7 Thursch, E., Szabo, G., Goupil, J.M., Chambellan, A. and Cornet, D. *J. Chim. Phys.* 1982, **79**, 479
8 Miedzinska, K.M. and Hollebone, B.R. *Can. J. Chem.* 1986, **64**, 1382
9 (a) Wichterlova, B., Tvaruzkova, Z. and Novakova, J. *J. Chem. Soc., Faraday Trans. 1* 1983, **79**, 1573. (b) Beran, S., Jiru, P. and Wichterlova, B. *J. Chem. Soc., Faraday Trans. 1* 1983, **79**, 1585. (c) Tvaruzkova, Z. and Wichterlova, B. *J. Chem. Soc., Faraday Trans. 1* 1983, **79**, 1591
10 Pearce, J.R. and Mortier, W.J. *J. Chem. Soc., Faraday Trans. 1* 1981, **77**, 1935
11 Shpiro, E.S., Tulecova, G.J., Zaikovskii, V.I., Tkachenko, O.P., Vasina, T.V., Bragin, O.V. and Minachev, K.K.M., in *Zeolites as Catalysts, Sorbents and Detergent Builders* (Eds. H.G. Karge and J. Weitkamp) Elsevier, Amsterdam, 1989
12 Kellerman, R. and Klier, K., in *Molecular Sieves – II* (Ed. J.R. Katzer) American Chemical Society, Washington, DC, 1977, p. 120
13 Coughlan, B., McCann, W.A. and Carroll, W.M. *Chem. Ind.* 1977, 358
14 Pearce, J.R., Sherwood, D., Hall, M.B. and Lunsford, J.H. *J. Phys. Chem.* 1980, **84**, 3215
15 Yashima, T., Nagata, J., Shimazaki, Y. and Hara, N., in *Molecular Sieves – II* (Ed. J.R. Katzer) American Chemical Society, Washington, DC, 1977, p. 626
16 Voght, F., Bremer, H., Rubinstejn, A.M., Dasevskij, M.I., Slinkin, A.A. and Kljacko, A.L. *Z. Anorg. Allg. Chem.* 1976, **423**, 155
17 Kellerman, R., Hutta, P.J. and Klier, K. *J. Am. Chem. Soc.* 1974, **96**, 5946
18 Mikheikin, I.D., Zhidomirov, G.M. and Kazanskii, V.B. *Russ. Chem. Rev.* 1972, **41**(5), 468
19 Atanasova, V.D., Shvets, V.A. and Kazanskii, V.B. *Kinet. Katal.* 1977, **18**, 1033
20 Munuera, G. and Rives, V., in *Proceedings of the Vth Ibero-American Symposium on Catalysis*, 1978, Vol. 1, p. 101
21 (a) Weckhuysen, B.M., De Ridder, L.M. and Schoonheydt, R.A. *J. Phys. Chem.* 1993, **97**, 4756; (b) Weckhuysen, B.M., Verberckmoes, A.A., Buttiens, A.L. and Schoonheydt, R.A. *J. Phys. Chem.* 1994, **98**, 579
22 Schoonheydt, R.A., in *Spectroscopy in Heterogeneous Catalysts* (Ed. F. Delannay) Marcel Dekker, New York, Basel, 1984, Chap. 4
23 McDaniel, M.P. *Adv. Catal.* 1985, **33**, 47
24 Corma, A., Sastre, G., Viruela, R. and Zicovich-Wilson, C. *J. Catal.* 1992, **136**, 521
25 (a) Lievens, J.L., PhD Thesis #229, Faculty of Agronomy, K.U.Leuven, 1992; (b) Lievens, J.L., Mortier, W.J. and Verduijn, J.P. *J. Phys. Chem.* 1992, **96**, 5473